Original Article

MOLECULAR METABOLISM

Brown adipocytes can display a mammary basal myoepithelial cell phenotype *in vivo*

Li Li [1,2,5], Baoguo Li [1,2,5], Min Li [1,2], Chaoqun Niu [1], Guanlin Wang [1,2], Ting Li [1], Elżbieta Król [3], Wanzhu Jin [4], John R. Speakman [1,3,*]

ABSTRACT

Objective: Previous work has suggested that white adipocytes may also show a mammary luminal secretory cell phenotype during lactation. The capacity of brown and beige/brite adipocytes to display a mammary cell phenotype and the levels at which they demonstrate such phenotypes *in vivo* is currently unknown.

Methods: To investigate the putative adipocyte origin of mammary gland cells, we performed genetic lineage-labeling experiments in BAT and the mammary glands.

Results: These studies indicated that the classic brown adipocytes (Ucp1^{+}) and subcutaneous beige/brite adipocytes (Ucp1$^{-/+}$) were found in the mammary gland during lactation, when they exhibited a mammary myoepithelial phenotype. Up to 2.5% of the anterior dorsal interscapular mammary myoepithelial cell population had a brown adipocyte origin with an adipose and myoepithelial gene signature during lactation. Eliminating these cells, along with all the brown adipocytes, significantly slowed offspring growth, potentially demonstrating their functional importance. Additionally, we showed mammary epithelial lineage Mmtv^{+} and Krt14^{+} cells expressed brown adipocyte markers after weaning, demonstrating that mammary gland cells can display an adipose phenotype.

Conclusions: The identification of a brown adipocyte origin of mammary myoepithelial cells provides a novel perspective on the interrelationships between adipocytes and mammary cells with implications for our understanding of obesity and breast cancer.

Keywords Brown adipocytes; Mammary gland; Lactation; Basal myoepithelial cells; Beige/brite adipocytes

1. INTRODUCTION

Early research suggested that there are two types of adipocytes: white and brown [1]. White adipocytes store excess energy intake as a large unilocular lipid droplet. In contrast, brown adipocytes have much smaller multilocular lipid droplets, and abundant mitochondria. Brown adipocytes generate heat via activation of uncoupling protein 1 (UCP1) that resides on the inner mitochondrial membrane, and acts by decoupling proton transfer across the membrane from synthesis of ATP [1]. More recently, it has been demonstrated that a unique lineage of cells, called 'brown in white (brite)' [2] or 'beige' [3] adipocytes, have the capacity to show both brown and white phenotypes under different conditions. These beige/brite cells originate from special adipocyte precursor cells, which are distinct from white adipocyte precursor cells [3]. Furthermore, classic brown adipocytes arise from a Myf5^{+}/Pax7^{+} skeletal muscle stem cell origin [4–7], but a recent study suggested that Myf5^{+} is a location marker rather than a marker of a specific cell lineage [8–10]. Hence, the current classification of 'fat' cells includes three main types: white adipocytes with an exclusively white phenotype, brown (Ucp1^{+}) adipocytes from the muscle lineage that can only exhibit the brown phenotype, and 'beige/brite' (Ucp1$^{-/+}$) adipocytes that can show both phenotypes [11].

The mammary gland is a milk producing exocrine gland. The mammary duct is composed of several cell lineages including an inner layer of secretory- or ductal-like luminal epithelial cells (Krt8^{+}/Krt18^{+}) that secrete milk and an outer layer of smooth muscle-like basal myoepithelial cells (Krt14^{+}/Krt5^{+}), which contract the inner mammary ducts in response to the hormone oxytocin, facilitating milk letdown [12–14]. In virgin female mice, the mammary gland already has rudimentary ductal structures in the anterior and posterior subcutaneous white adipose tissues. During pregnancy, the proliferation of mammary myoepithelial (Lin^{-}:CD24^{+}:CD29^{hi}) and luminal (Lin^{-}:CD24^{+}:CD29^{low}) stem cells located in the mammary ductal terminal end buds (TEB) facilitates the branching and development of the mammary duct, These ducts gradually penetrate and substitute almost all of the subcutaneous fat pads [15–17].

An often neglected aspect of adipocyte biology is the suggestion that, in female mice, white adipocytes might be capable of

[1]State Key Laboratory of Molecular Developmental Biology, Institute of Genetics and Developmental Biology, Chinese Academy of Sciences, Beijing, 100101, China [2]University of Chinese Academy of Sciences, Beijing, 100049, China [3]Institute of Biological and Environmental Sciences, University of Aberdeen, Aberdeen, Scotland, UK [4]Key Laboratory of Animal Ecology and Conservation Biology, Institute of Zoology, Chinese Academy of Sciences, Beijing, China

[5] Li Li and Baoguo Li contributed equally to this work.

*Corresponding author. State Key Laboratory of Molecular Developmental Biology, Institute of Genetics and Developmental Biology, Chinese Academy of Sciences, Beijing, 100101, China. E-mail: j.speakman@genetics.ac.cn (J.R. Speakman).

Received July 26, 2017 • Accepted July 31, 2017 • Available online 5 August 2017

http://dx.doi.org/10.1016/j.molmet.2017.07.015

transdifferentiation into mammary luminal secretory epithelium cells [18,19], sometimes called 'pink' adipocytes [20]. As these 'pink' adipocyte studies were performed prior to the discovery of the beige/brite lineage, it is unclear whether these transformed mammary gland cells were truly white or if they were beige/brite adipocytes presenting a white and then pink phenotype. Moreover, whether classic brown adipocytes might also be able to transform into mammary gland cells is unknown. This may be important because it was recently demonstrated that there is increased expression of brown and beige/brite adipocyte markers (MYF5 and UCP1) among breast cancer cells, that influences the formation of xenografts in mice [21]. Critically, depletion of Ucp1^{+} or Myf5^{+} cells significantly reduced tumor development. Thus, conversion of brown and beige/brite adipocytes into cells displaying a mammary gland phenotype may be an important contributor to the risk of developing breast cancer. It is currently unclear, however, whether brown and/or beige/brite adipocytes are able to transform into mammary gland cells. To answer this question, we performed multiple lineage labeling experiments in four different transgenic mouse models. We demonstrate that classic brown adipocytes, and probably beige/brite adipocytes, are capable of showing a mammary basal myoepithelium phenotype *in vivo*, but not a luminal secretory phenotype. Additionally, we show that if cells that express UCP1 are killed during lactation then the growth of their offspring is reduced, suggesting the conversion of brown/beige adipocytes to mammary cells is functionally significant, even though numerically small.

2. MATERIALS AND METHODS

2.1. Animals

All animal experiments were approved by the Institute of Genetics and Developmental Biology Chinese Academy of Sciences (IGDB-CAS) Institutional Animal Care and Use Committee (IACUC). All animals were housed in rooms kept at 23 ± 1 °C with a dark—light cycle of 12 h—12 h (lights on at 0730 h) and fed *ad libitum* with a standard low fat chow diet. *Myf5-Cre* mice were kindly donated by Dr Kuang and Dr Zhu. Ucp1-HBEGF/eGFP (Ucp1-DTR) and Ucp1-CreER mice were kindly donated by Dr Wolfrum. Tamoxifen induction of Cre activity was performed by gavaging 3 × daily 200 μL tamoxifen (10 mg/mL, Sigma—Aldrich) in sunflower oil when the animals were kept at 5 °C. *Ucp1-iCre* mice were built by Biocytogen. To avoid disrupting *Ucp1* expression, *IRES-Cre* was introduced between the coding sequence of exon 6 and the 3′UTR. The internal ribosome entry site (IRES) was used to allow UCP1 and iCRE expression at the same time with lower levels. To avoid disrupting the polyA signal of *Ucp1* expression, a Neo cassette flanked by frt sites was inserted 300 bp downstream of the 3′UTR. Heterozygous mice were healthy and fertile. We then crossed *Ucp1-iCre* mice with *Rosa-mTmG* reporter mice. Transgenic mice *Mmtv-Cre* (Stock #003553), *Krt14-Cre* (Stock #004782) and *Rosa-mTmG* reporter mice (Stock #007676) were purchased from the Nanjing Biomedical Research Institute of Nanjing University (NBRI), *Rosa-tdTomato* reporter mice were purchased from Vitalstar and the SCID-beige mice were purchased from Charles River.

2.2. Immunohistochemistry

Animals were perfused with 4% paraformaldehyde (PFA), and mammary gland or BAT were post-fixed by 4% PFA at 4 °C overnight and embedded with OCT after dehydration by 30% sucrose solution for 48 h. Twenty micrometer sections were cut using a Leica cryostat (CM3050S). Frozen sections were fixed in cold PFA for 20 min then rinsed in PBS three times. Then sections were incubated in blocking buffer (5% BSA/0.1% Triton in PBS) at room temperature for 1 h, primary antibodies were added in appropriate concentrations in staining buffer (1% BSA/0.1% Triton in PBS) at 4 °C overnight, followed by a wash and incubation with a secondary antibody for 1 h at room temperature. Nuclei were stained with DAPI (4′,6-diamidino-2-phenylindole). Fluorescence images of frozen sections were acquired on a FV1000 confocal microscope (Olympus) and cultured cell images were taken on a LSM780 confocal microscope (Zeiss).

2.3. Antibodies

The following primary antibodies were used: anti-GFP (rat, 1:2000, MBL), anti-GFP (rabbit, 1:1000, Abcam), anti-beta-Casein (goat, 1:200, Santa Cruz), anti-KRT14 (rabbit, 1:1000, Covance), anti-KRT14 (mouse, 1:1000, Thermo), anti-KRT5 (rabbit, 1:1000, Covance), anti-KRT5 (mouse, 1:1000, Thermo), anti-KRT8 (rabbit, 1:1000, Abcam), anti-E-cadherin (mouse, 1:1000, BD), anti-Perilipin1 (goat, 1:1000, Abcam), anti-PPAR-γ (rabbit, 1:1000, Cell Signaling Technology), anti-UCP1 (rabbit, 1:1000, Abcam), Deep red LipidTOX neutral lipid stain (1:500, Invitrogen). All secondary antibodies were Alexa Fluor-conjugated from Invitrogen: anti-mouse Alexa 647, anti-rabbit Alexa 647, anti-goat Alexa 647, anti-rat Alexa 488, anti-rabbit Alexa 488, anti-mouse Alexa 594, anti-rabbit Alexa 594, anti-goat Alexa 594, anti-rabbit Alexa 405.

2.4. Flow cytometry

Mammary cells were obtained as performed in earlier studies [15,22]. In brief, inguinal mammary gland or interscapular BAT samples were dissociated by scissors and then incubated with 5% fetal bovine serum containing collagenase (300 IU/mL, Sigma) and hyaluronidase (100 IU/mL, Sigma) for 60 min at 37°C. Samples were then centrifuged at 500 g for 5 min, and the cell fractions were incubated with 0.25% trypsin-EGTA for 3 min, then resuspended in Dispase (5 mg/mL, Sigma) and DNaseI (50 IU/mL, Takara) for 5 min, and red blood cell lysis (0.64% NH_4Cl) for 3 min before filtration through a 40 μm cell mesh. Antibodies were incubated in PBS with 5% FBS for 20 min. The following primary antibodies were used: Percp-cy5.5 conjugated anti-CD24 (eBioscience, Clone M1/69), APC conjugated anti-CD29 (eBioscience, Clone HMB1-1), PE-cy7 conjugated anti-CD31 (eBioscience, Clone 390), PE-cy7 conjugated anti-CD45 (eBioscience, Clone 30-F11). The positive antibody signals were gated based on fluorescence minus one (FMO) control every time. Cell sorting was performed on FACSAria, and the data were read using Flowjo7.6.1 software.

2.5. Administration of AAV vectors

The AAV2/9-CAG-DIO-mCherry (1.2×10^{12} vg/mL) was purchased from the HanBio company. The *Ucp1-iCre* mice were anesthetized with isoflurane. For interscapular BAT administration, a longitudinal skin incision at the interscapular region was performed, and each side of the BAT received three injections of 5 μL AAV solution.

2.6. Ucp1-GFP cell preparation and cell transplantation

Six-week-old virgin *Ucp1-iCre-ROSA^{mTmG}* female mice were anesthetized with isoflurane. Interscapular BAT was removed and minced into small pieces then incubated with 5% fetal bovine serum containing collagenase (300 IU/mL, Sigma) and hyaluronidase (100 IU/mL, Sigma) for 30 min at 37 °C before filtration through a 100 μm cell mesh. Floating adipocytes were collected by a syringe, and mature brown adipocytes (DAPI negative) were sorted by 130 mm diameter nozzle to exclude the debris and other unrelated cells using BD Bioscience Aria sorter according to a recent study [11]. The Ucp1-GFP positive suspension was mixed with 0.9% germ-free sodium chloride and injected into one side of the inguinal fat pad of recipient 8-week-old female SCID-beige mice. After the surgery, mice were injected with

penicillin (2000 units per day) for the subsequent three days. After 3 days of recovery, the recipient mice were mated with an age-matched wild type BALB/c male mice.

2.7. Diphtheria toxin injection

Wild type or Ucp1-DTR mice were subcutaneously injected with DT ([Sigma], 400 ng per mouse, diluted in PBS) under the skin of the scapular region twice a day for every 3 days.

2.8. Protein analysis

The BAT tissue was homogenized in T-PER tissue protein extraction reagent buffer ([Thermo], supplement with protease inhibitor [Sigma] and PMSF [Sigma]). The protein concentration was determined by the BCA method [Thermo]. The protein samples were separated by a 12% SDS-polyacrylamide gel then electrotransferred to PVDF membranes [Millipore]. Primary antibody for UCP1 (rabbit, 1:5000, Abcam) was detected by the HRP conjugated anti-rabbit secondary antibody.

2.9. NE induced oxygen consumption

O_2 consumption and CO_2 production were determined by indirect calorimetry using a Servomex 4100 analyzer linked to a mass flow controller. Measurements of O_2 and CO_2 in the outflow gas stream were measured every 30 s. Each animal was housed and calmed in the gas collection chamber at least 3 h before NE injection to obtain basal O_2 consumption and CO_2 production before Norepinephrine (1.2 mg/kg body weight) was injected subcutaneously in the dorsal scapular region [23].

2.10. RNA-seq and bioinformatics

Mature brown adipocytes were sorted by 130 mm diameter nozzle, and mammary myoepithelial cells were sorted by 70 mm diameter nozzle using BD Bioscience Aria sorter. 10,000–20,000 (DAPI negative) living cells per individual were collected in lysis buffer and total RNA were extract immediately by RNeasy Micro Kit (Qiagen) according to manufacturer's recommendations. The amplified cDNA samples were prepared by the SMART-Seq™ v4 Ultra™ Low Input RNA Kit for Sequencing (Clontech) and validated by the Agilent 2100 Bioanalyzer. Sequencing libraries were generated using NEBNext® Ultra™ DNA Library Prep Kit for Illumina® (NEB, USA) and 150 bp paired-end reads were sequenced on Illumina Hiseq2500 platform in Novogene company. Full sequencing data are available online at NCBI GEO (GSE93230). The paired-end clean reads were aligned to the reference genome using TopHat and each gene reads numbers were count by HTseq. Differential expression gene (DEG) analysis was performed by DEseq2 package in which gene length and dispersion bias was corrected. The resulting P-values were adjusted using the Benjamini and Hochberg's approach for controlling the false discovery rate (FDR). Genes with an adjusted P-value <0.05 found by DESeq2 were assigned as differentially expressed.

2.11. Cell culture

SVF cells of inguinal adipose tissue from *Krt14-Cre-ROSA*^{mTmG} mice were maintained for 1 week in growth medium (DMEM: F12 supplemented with 5% FBS, 5 μg/mL insulin, 500 ng/mL hydrocortisone, 10 ng/mL epidermal growth factor and 1% penicillin-streptomycin). Adipogenic differentiation was induced by induction media (DMEM with 10% FBS, 0.125 mM indomethacin [Sigma], 0.5 mM isobutylmethylxanthine [Sigma], 2 μg/mL dexamethasone [Sigma], 1 μM rosiglitazone [Sigma], 5 μg/mL insulin [Sigma], 1 nM triiodothyronine [Sigma]) for 2 days. Over the next 4 days, cells were maintained in differentiation media (1 μM rosiglitazone, 5 μg/mL insulin, 1 nM triiodothyronine) until harvest. For cAMP agonist stimulation, cells were treated with 10 μM Forskolin [Sigma] or DMSO for 6 h before harvesting.

2.12. Quantification of number and size of GFP cell in mammary gland and adipose tissue

A minimum of three mice were analyzed per condition by FACS or immunohistochemistry. A minimum of 200 GFP$^+$ clones per condition were counted in mammary gland respectively. KRT14 expressing basal myoepithelial cells and KRT8 expressing luminal cells in GFP$^+$ cells were scored. The clones were grouped into three classes by cell size: single cell, two to four cells, and more than four cells. A minimum of 500 Perilipin1$^+$ or LipidTox$^+$ adipocytes per stage per animal were counted for Krt14$^+$ or Mmtv$^+$ adipocytes in adipose tissue respectively.

2.13. Quantitative real-time PCR (qPCR)

The total RNA of sorted cells was isolated by TRIzol (Invitrogen) and cDNA synthesis was performed by M-MLV Reverse Transcriptase (Invitrogen) under manufacturer's recommendations. The real-time PCR was analyzed using Tip Green qPCR Super Mix (TransGen Biotech) with Mx3005P Real-Time PCR System (Agilent). qPCR values were normalized by *Tbp* mRNA expression. Primer sequences are available in Table S4.

2.14. Milk energy output (MEO)

Daily energy expenditure (DEE) of the lactation mice were measured by the doubly labelled water (DLW) technique on days 14–16 of lactation. MEO was calculated from the difference between metabolic food energy intakes and DEE [24].

2.15. Statistical analysis

Data are presented as mean ± s.e.m. Cell numbers are presented to 2 significant figures. Unless stated otherwise, an unpaired two-sided Student's *t*-test was used for comparisons with $^*P < 0.05$ and $^{**}P < 0.01$ compared with control group.

3. RESULTS

3.1. Some Myf5$^+$ cells from the interscapular brown adipose tissue display a myoepithelial phenotype during lactation

Previous studies have shown that white adipocytes can transdifferentiate into mammary secretory-like cells during pregnancy and lactation [18,19]. In addition, other studies have indicated that the thermogenic capacity of BAT is suppressed during lactation in mice [24,25]. It is unclear whether these two changes are in some way linked, as might for example happen if brown adipocytes were also transdifferentiating into mammary gland cells. To determine whether classic brown adipocytes are involved in mammary gland development, we used *Myf5-Cre-ROSA*^{mTmG} transgenic mice. *Myf5* is a transcription factor that plays a major role in skeletal muscle differentiation and myogenesis [26,27], and classic brown adipocytes share the skeletal muscle origin from the embryonic stage [4,28–30]. We crossed *Myf5-Cre* transgenic mice with *Rosa-mTmG* reporter mice. The mTmG mice express a double fluorescent protein on the cell membrane, and the loxp-stop-loxp tdTomato cassette is replaced by enhanced GFP, after CRE-mediated recombination [31]. Hence, cells currently or previously expressing *Myf5* become GFP-positive on the cell surface, while other cells not expressing GFP remain Tomato positive on the cell surface, allowing us to monitor the potential adipocyte ancestry of mammary gland cells. Since *Myf5-Cre* labels brown adipocyte in an anatomical way, samples in this experiment were carefully chosen from the interscapular region as brown adipose tissue (Figure S1A).

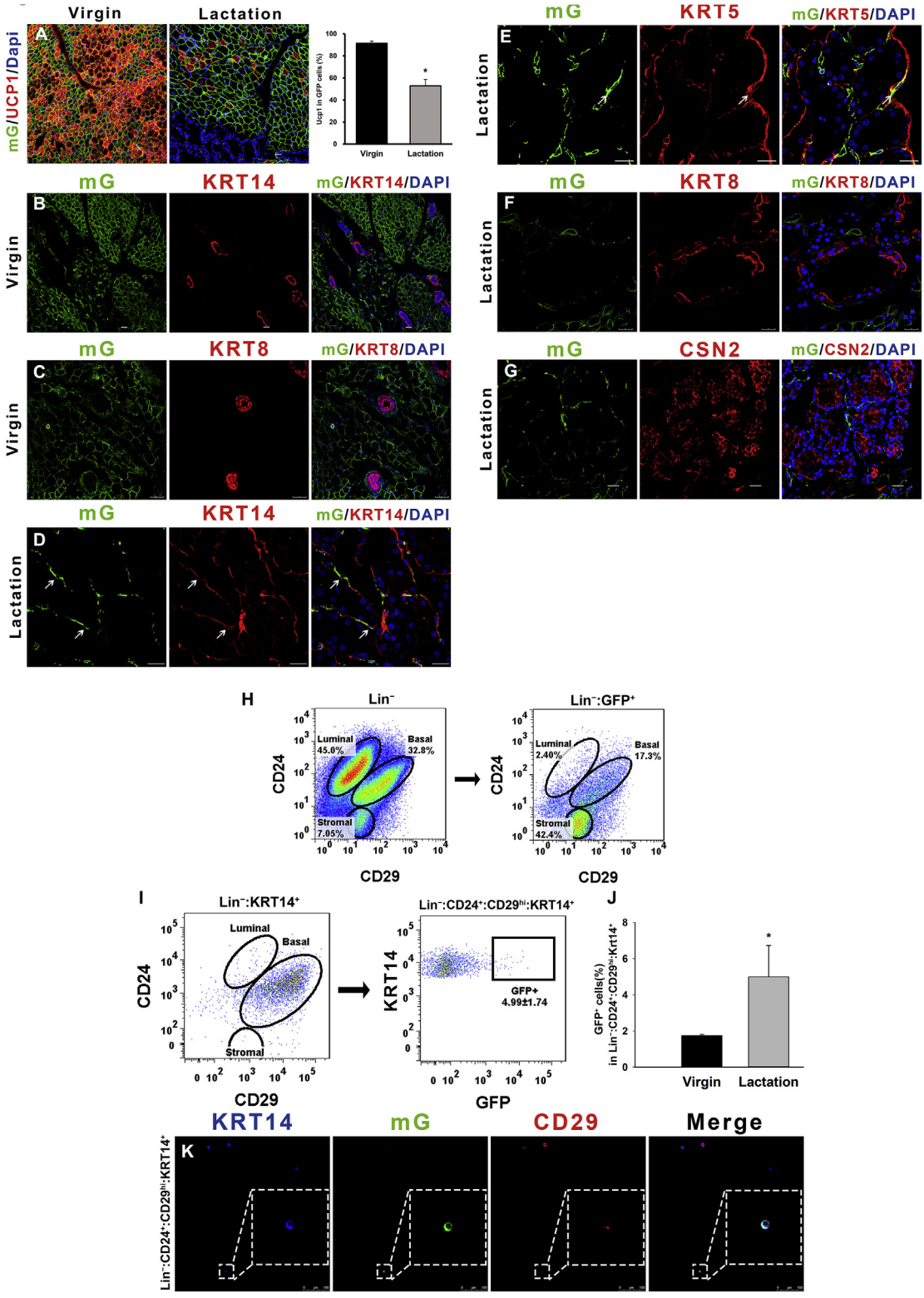

Figure 1: Myf5-GFP cells could convert into mammary basal myoepithelial cells during the reproductive stage. (A) The UCP1 expression level in BAT during lactation (middle) compared to the virgin state (left). The percentage of UCP1 expression in Myf5-GFP cells shows in histogram (right). (B and C) In the virgin stage of the *Myf5-Cre-ROSA*^{mTmG} mice, the interscapular BAT was stained for mammary markers KRT14 and KRT8. (D and E) During lactation, Myf5-GFP cells in the scapular region expressed the mammary basal myoepithelial markers KRT14 and KRT5. (F and G) Myf5-GFP cells were negative for the mammary luminal markers KRT8 and CSN2. (H) Flow cytometry analysis of CD24 and CD29 of Lin^{-} cells showing Myf5-GFP expression in the anterior dorsal interscapular region mammary basal cell populations. (I and J) The Myf5-GFP cells percentage in KRT14^{+} mammary basal myoepithelial population (defined as Lin^{-}:CD24^{+}:CD29^{hi}:Krt14^{+}) during lactation (I) and virgin stage (n = 3) (J). (K) The Krt14^{+} mammary basal myoepithelial population were sorted out to observe Myf5-GFP cells. Scale bar: 20 μm. The data represent means + s.e.m. *P <0.05.

Up to 91% interscapular Myf5-GFP cells were UCP1 positive in the virgin state, suggesting that the *Myf5-Cre-ROSA*^{mTmG} transgenic model is suitable to label the classic brown adipose tissue, although there are clearly other cells (about 9%) expressing Myf5 that are not UCP1 positive. The number of UCP1 positive Myf5-GFP cells dropped to 52% during lactation (Figure 1A), which suggests that BAT thermogenesis during lactation was suppressed, consistent with our previous studies [24]. In the virgin stage of the *Myf5-Cre-ROSA*^{mTmG} mice, Myf5-GFP positive classic brown adipocytes in the interscapular region did not express the mammary markers KRT14 (myoepithelial) or KRT8 (luminal), and the mammary gland did not contain GFP cells under immunostaining analyses (Figure 1B and C). During lactation, the anterior mammary gland enlarged onto the dorsal surface and invaded the BAT in the interscapular region (Figure S1B), indicating that the mammary gland and BAT are often in close contact in this region. As well as the typical spherical fat cell shape, some of the Myf5-GFP cells also presented a slender shape and together several cells formed a basket-like structure (Figure 1D and E) during both pregnancy and lactation, relative to non-reproductive age-matched *Myf5-Cre-ROSA*^{mTmG} mice. Myf5-GFP cells contained mammary basal myoepithelial markers as revealed by co-expression of GFP with KRT14 and Keratin 5 (KRT5) in the dorsal part of the interscapular mammary gland (Figure 1D and E). However, most of the slender Myf5-GFP cells were in close proximity to mammary luminal KRT8 and CSN2 positive cells, but did not co-stain for these markers (Figure 1F and G), suggesting that Myf5-GFP cells did not display a luminal secretory cell phenotype. Clonal analysis of Myf5-GFP mammary clones suggested that all the clones were basal clones (Figure S1C), which contained about 27.3%—43.3% single basal clones. A small number of Myf5-GFP cells were found in the posterior inguinal mammary gland of the *Myf5-Cre-ROSA*^{mTmG} mice in both virgin and lactation stages, but these Myf5-GFP cells did not contain mammary cell markers KRT14 or KRT8 by immunostaining analysis (Figure S1D—G).

To monitor the dynamics of the Myf5-GFP cell content in the mammary gland, the stromal vascular fraction (SVF) cells in the interscapular and inguinal fat pads were isolated from the *Myf5-Cre-ROSA*^{mTmG} mice for flow cytometry analysis (Figure S1H). The positive GFP signal was gated by fluorescence minus one (FMO) control of the wild type mouse (Figure S1I). Quantification of the labeling events by FACS analysis [14,15] indicated that Myf5-GFP cells were found in the mammary basal myoepithelial populations (Lin$^-$:CD24$^+$:CD29^{hi}), but not the luminal populations (Lin$^-$:CD24$^+$:CD29^{low}), in the interscapular region of 8-week-old virgin female mice as well as in pregnant and lactating female mice (Figure 1H). To exclude the possibility that there are potential adipose precursors in the mammary basal myoepithelial population (Lin$^-$:CD24$^+$:CD29^{hi}), we combined the mammary myoepithelial cytoplasmic marker KRT14 with the cell surface markers (details in Figure S3C). The KRT14-positive cells were predominantly scattered among the mammary basal myoepithelial population (Lin$^-$:CD24$^+$:CD29^{hi}) (Figure 1I and S3C). On average, 5.0 ($\pm$1.7) % of the selected KRT14 positive mammary basal myoepithelial population (Lin$^-$:CD24$^+$:CD29^{hi}:KRT14$^+$) were found to be Myf5-GFP positive in the interscapular region of the *Myf5-Cre-ROSA*^{mTmG} mice during lactation (Figure 1I and J) and 1.7 ($\pm$0.1) % of KRT14 positive basal myoepithelial population (Lin$^-$:CD24$^+$:CD29^{hi}:KRT14$^+$) were found to be Myf5-GFP positive in the virgin stage. In addition, the KRT14 positive basal myoepithelial population (Lin$^-$:CD24$^+$:CD29^{hi}:KRT14$^+$) were sorted and Myf5-GFP cells were confirmed by confocal microscopy (Figure 1K). It is unclear whether the Myf5$^+$ progenitor cells were recruited to become mammary myoepithelial cells, or whether the mature brown adipocytes transdifferentiated into mammary basal myoepithelial cells. However, given the characteristics of *Myf5-Cre*, it is also possible that Myf5-GFP also labeled some anterior region mammary lineage cells. Hence, while these data are consistent with classic brown adipocytes showing a myoepithelial cell phenotype in lactation, they are not definitive, since Myf5 was not exclusively expressed in brown adipocytes. In contrast to the anterior dorsal mammary gland, only 0.01 ($\pm$0.04) % of the posterior mammary Lin$^-$:CD24$^+$:CD29^{hi}:KRT14$^+$ population were Myf5-GFP positive during lactation suggesting that the Myf5-GFP cells in the inguinal region did not contribute to the development of mammary myoepithelial cells (Figure S1K). Furthermore, the gene expression level of *Myf5* was validated by Q-PCR, indicating that *Myf5* was not expressed in FACS sorted Myf5-GFP brown adipocytes or myoepithelial cells but was expressed in skeletal muscle (Figure S1L). These data indicated that the Myf5-GFP cells (only) in the interscapular brown adipose region can exhibit a mammary basal myoepithelial cell phenotype, but they did not display a luminal cell phenotype during lactation.

3.2. Ucp1$^+$ brown and beige/brite adipocytes can show a mammary myoepithelial cell phenotype

In the light of the potential adipocyte origin and presence of the Myf5$^+$ progenitor heritage in some mammary basal myoepithelial cells, we further explored whether mature brown adipocytes expressing UCP1 also shared this phenotype. UCP1 is the hallmark gene regulated by ambient temperature and expressed in mature brown and beige/brite adipocytes [32,33]. We generated an *Ucp1-IRES-Cre* transgenic mouse to trace mature brown cells. To also track beige/brite adipocytes in inguinal adipose tissue, *Ucp1-iCre-ROSA*^{mTmG} female mice were cold exposed at 5 °C for 7 days before mating. Both membrane GFP and UCP1 signals were observed in interscapular brown adipose tissue and inguinal adipose tissue (Figure 2A and S2A). Consistent with the *Myf5-Cre-ROSA*^{mTmG} model, 95% of interscapular Ucp1-GFP cells were UCP1 positive during the virgin stage and the UCP1 positive percentage dropped to 41% during lactation (Figure 2A). Mature brown adipocytes and beige/brite adipocytes did not express the mammary markers KRT14 or KRT8, and the KRT14/KRT8 positive mammary gland cells did not include Ucp1-GFP cells during the virgin stage (Figure 2B and C). Consistent with the *Myf5-Cre-ROSA*^{mTmG} model, during lactation, the Ucp1-GFP cells were found in both the interscapular (Figure 2D and E) and inguinal (Figure 2F and G) mammary glands. The Ucp1-GFP cells expressed low levels of KRT14 and KRT5 compared to neighboring basal myoepithelial cells and none of Ucp1-GFP cells expressed the mammary luminal marker KRT8 (Figure S2B).

FACS analysis of the SVF from *Ucp1-iCre-ROSA*^{mTmG} female mice showed that Ucp1-GFP cells in both the anterior and posterior mammary glands were only observed in the mammary basal myoepithelial populations (Figure 2H and I), rather than in the luminal or stromal cells, which was consistent with the result for Myf5-GFP cells (above). On average, 2.2 ($\pm$0.1) % of the sorted KRT14 positive mammary basal myoepithelial population (Lin$^-$:CD24$^+$:CD29^{hi}:KRT14$^+$) in the anterior dorsal interscapular region (Figure S1A) were Ucp1-GFP positive during lactation, but only 0.13 ($\pm$0.06) % were GFP positive in the virgin stage (*t*-test, $t_3 = 15.22$, $p < 0.05$) (Figure 2J and K). The KRT14 positive basal myoepithelial population (Lin$^-$:CD24$^+$:CD29^{hi}:KRT14$^+$) were sorted out and Ucp1-GFP cells were confirmed by confocal microscopy (Figure 2L). The difference in the percentage of Ucp1-GFP cells in the mammary basal myoepithelial population (Lin$^-$:CD24$^+$:CD29^{hi}:KRT14$^+$) between the two stages indicated that the conversion between brown adipocytes and mammary myoepithelial cells might happen during the reproductive stage.

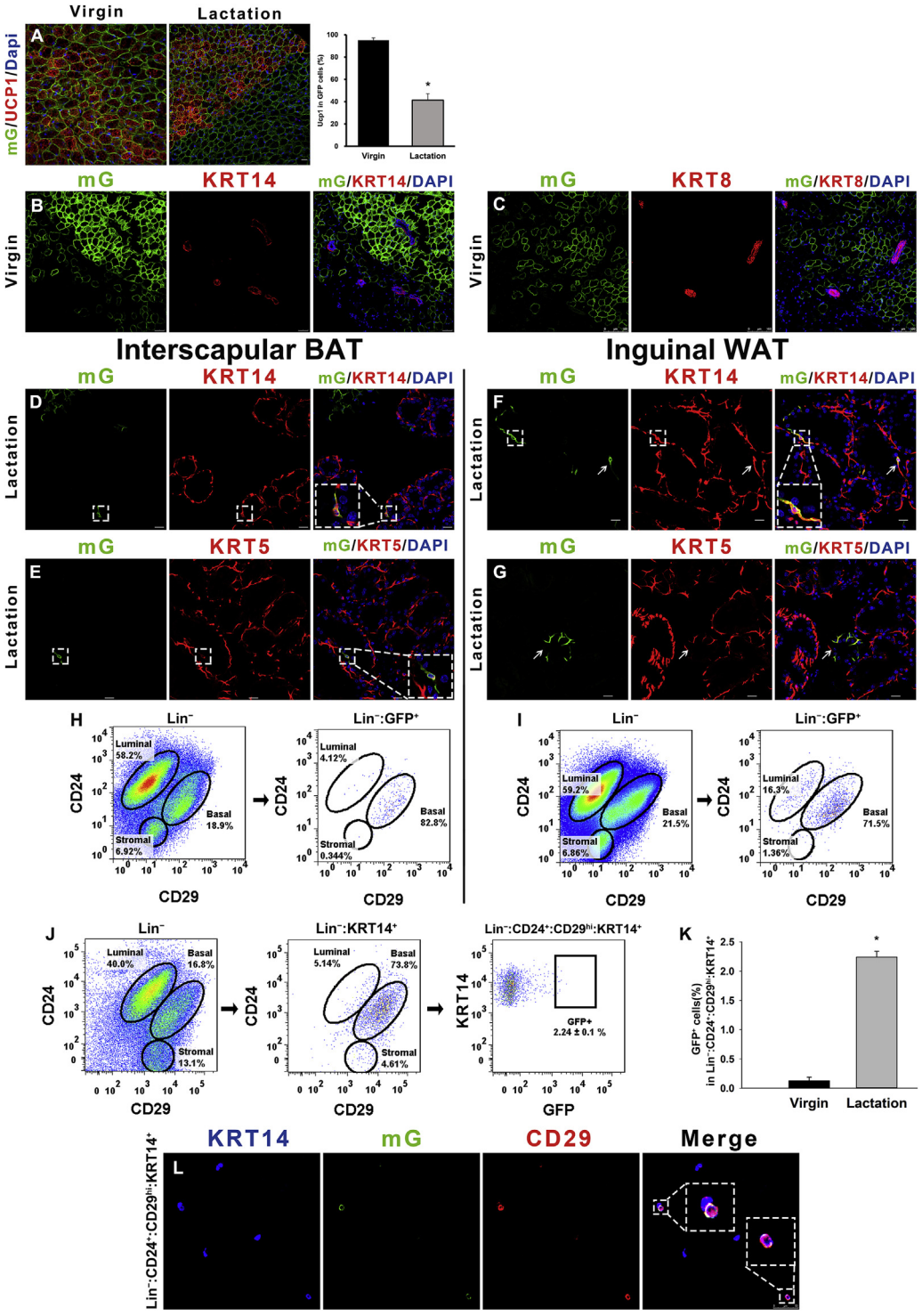

Figure 2: Ucp1-GFP cells convert into mammary basal myoepithelial cells during the reproductive stage. (A) The UCP1 expression level in BAT during lactation (middle) compared to the virgin state (left). The percentage of UCP1 expression in Ucp1-GFP cells are shown in the histogram (right). (B and C) In the virgin stage of the *Ucp1-Cre-ROSA*^{mTmG} mice, the interscapular BAT was stained for mammary markers KRT14 and KRT8. (D–G) During lactation, Ucp1-GFP cells contain mammary basal myoepithelial markers KRT14 and KRT5 in the dorsal region of the anterior mammary gland (D and E) and the posterior mammary gland (F and G). (H and I) Flow cytometry analysis of CD24 and CD29 of Lin$^-$ cells showing Ucp1-GFP expression in mammary basal myoepithelial cell populations in the dorsal region of the anterior interscapular mammary gland (H) and the posterior inguinal mammary gland (I). (J and K) The Ucp1-GFP cell percentage in Krt14$^+$ mammary basal myoepithelial population (defined as Lin$^-$:CD24$^+$:CD29^{hi}:Krt14$^+$) during lactation (J) and virgin stage (both n = 3) (K). (L) The Krt14$^+$ mammary basal myoepithelial population were selected to observe Ucp1-GFP cells. (M) Schematic diagrams of Ucp1-GFP cell transplantation experiments using the SCID-beige mice are shown in M. (N–P) During lactation day 5, the inguinal mammary gland from the Ucp1-GFP cells grafted SCID-beige female mice were sectioned and immunostained for mammary markers KRT14, KRT5 and KRT8. (Q) Schematic diagrams of lineage-tracing experiments using *Ucp1-CreER-ROSA*^{tdTomato} mice are shown in Q. (R–U) Interscapular brown adipose depots and inguinal mammary gland from lactation *Ucp1-CreER-ROSA*^{tdTomato} mice were sectioned and immunostained for RFP, Perilipin1 and mammary markers KRT14 and KRT5. Scale bar: 20 μm. The data represent means + s.e.m. *P <0.05.

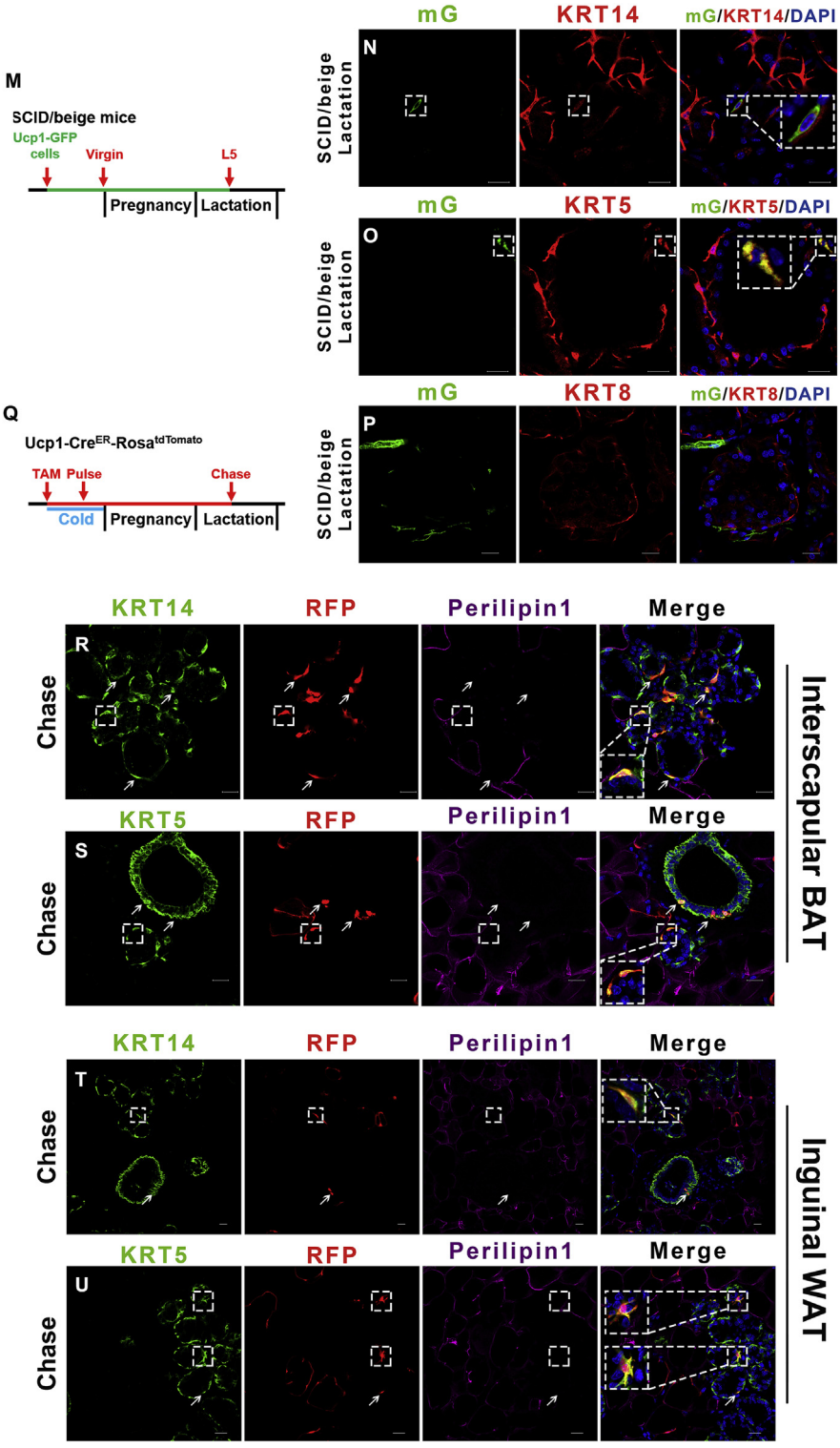

Figure 2: (*continued*).

To further investigate the relationship between the mature brown adipocytes and the mammary myoepithelial cells, we performed a fate-mapping study using DIO-mCherry adeno-associated virus (AAV) with *Ucp1-iCre* mice. The DIO-mCherry AAV carries a reversed loxp-mCherry-loxp cassette, resulting in expression of mCherry only after Cre-mediated recombination (Figure S2C). The 8-week-old *Ucp1-iCre* female mice were cold stimulated at 5 °C for 4—5 days, immediately after the interscapular injection of the DIO-mCherry AAV (Figure 2D). After this pulse-labeling period, *Ucp1-iCre* mice were housed at room temperature with males to get pregnant. The *Ucp1-iCre* mice were sacrificed on day 2 of lactation for a 25-day AAV chasing period. Large numbers of brown multiocular adipocytes (Perilipin1^{+}) were co-

expressing UCP1 and mCherry, and the white unilocular adipocytes (Perilipin1$^+$) were negative for UCP1 and mCherry, suggesting that the DIO-mCherry AAV specifically labeled the classic brown adipocytes in *Ucp1-iCre* mice after the injection (Figure S2E). The Ucp1-mCherry cells did not contain mammary cell markers KRT14 and KRT8 in the virgin stage during cold exposure (Figure S2F and G). During lactation, the Ucp1-mCherry cells expressed mammary basal myoepithelial markers KRT14 and KRT5 but not the mammary luminal marker KRT8 (Figure S2H–J). The presence of Ucp1-mCherry derived mammary basal myoepithelial cells during lactation indicates that mature brown adipocytes can directly convert into mammary basal myoepithelial cells in the reproductive mammary microenvironment.

To evaluate whether this conversion of brown adipocytes could continue without the microenvironment and sympathetic nervous system of the brown adipose tissue, we performed a cell xenograft experiment using a suspension of isolated Ucp1-GFP positive brown adipocytes from 6-week-old *Ucp1-iCre-ROSA*^{mTmG} female mice. The single alive cell suspension of mature brown adipocytes was obtained by FACS (Figure S6A and B) [11]. This suspension was injected into the inguinal fat pad of 8-week old SCID-beige female mice (Figure 2M). The immunocompromised SCID-beige mice possesses both autosomal recessive mutations SCID (*Prkdc*^{scid}) and beige (*Lyst*^{bg}), resulting in immunodeficiency affecting both the B and T lymphocytes and natural killer (NK) cells [34,35]. Such mice are able to tolerate the exogenous Ucp1-GFP cells through the pregnancy and lactation period. Due to limited space in the inguinal adipose tissue, only 10,000 Ucp1-GFP cells were injected into the fat pad in each SCID-beige mouse. After a three-day recovery from the surgery, 98% of the grafted Ucp1-GFP cells still expressed the adipose marker Perilipin1, and 30% of the GFP cells retained the multiocular brown adipocyte phenotype (Figure S3A), but the grafted Ucp1-GFP cells lost the UCP1 signal in the inguinal region (Figure S3B). This phenotype has also been reported in several previous BAT grafting experiments [36–39] suggesting the local microenvironment and sympathetic nervous system are vital to sustaining the expression level of UCP1 in the grafted cells. Consistent with the *Ucp1-iCre-ROSA*^{mTmG} model and the AAV experiments, the mammary cell markers Keratin 14 (KRT14, myoepithelial cells) and Keratin 8 (KRT8, luminal cells) were not expressed in the Ucp1-GFP cells of the SCID-beige mice (Figure S3C and D). The recipient SCID-beige mice were co-housed with male mice until late pregnancy. During lactation day 5, some of the grafted Ucp1-GFP$^+$ cells became slender, delipidized, and adjoined to the outer ring of mammary gland lobules, and up to 1.2 ($\pm$0.1)% of the total Ucp1-GFP cells expressed the mammary myoepithelial cell markers KRT14 and KRT5 in 5/6 SCID-beige mice (Figure 2N and O). The Ucp1-GFP cells did not express the luminal cell marker KRT8 (Figure 2P) in lactating SCID-beige mice, suggesting the brown adipocyte conversion is directed towards mammary myoepithelial cells rather than luminal cells and also independent of the brown adipose microenvironment.

To investigate whether the small proportion of Ucp1$^+$ myoepithelial cells from the *Ucp1-iCre* mice is due to spurious CRE activity, we performed a fate-mapping study using a different *Ucp1-CreER* mice line mated with *ROSA*^{tdTomato} mice [11]. The 8-week old *Ucp1-CreER-ROSA*^{tdTomato} female mice were cold stimulated at 5 °C for 3 days to activate brown and beige/brite adipocytes and tamoxifen was administered during this cold exposure period (Figure 2Q). After this pulse-labeling period, *Ucp1-CreER-ROSA*^{tdTomato} mice were housed at room temperature with males to get pregnant. The *Ucp1-CreER-ROSA*^{tdTomato} mice were sacrificed on day 1 of lactation for a 25–30 day chasing period. Similar to the DIO-AAV result, large numbers of brown multiocular adipocytes (Perilipin1$^+$) were detected co-expressing UCP1 and RFP, and the white unilocular adipocytes (Perilipin1$^+$) were negative for UCP1 and RFP, suggesting that the RFP specifically labeled the classic brown adipocytes in these *Ucp1-CreER-ROSA*^{tdTomato} mice (Figure S4A). The Ucp1-RFP cells did not contain mammary cell markers KRT14 and KRT8 in the virgin stage during cold exposure (Figure S4B and C). During lactation, the Perilipin1 negative Ucp1-RFP cells were slender and 98% contained the mammary basal myoepithelial markers KRT14 and KRT5 in both the interscapular and inguinal mammary gland (Figure 2R–U). The presence of Ucp1-RFP derived mammary basal myoepithelial cells during lactation indicates that mature brown adipocytes can convert into mammary basal myoepithelial cells in the reproductive mammary microenvironment.

To explore whether the Ucp1$^+$ expressing cells contribute to lactation performance, we selectively depleted the Ucp1$^+$ cells through the injection of diphtheria toxin (DT) into *Ucp1* promoter driven HBEGF/eGFP mice (Ucp1-DTR mice) [11]. UCP1 protein in the interscapular BAT was not detected after 3 days of DT injection (Figure S5A). To test the treatment of DT in every 3 days is enough to deplete the brown adipocytes, DT treated Ucp1-DTR mice were chronic cold stimulation for 7 days and the non-shivering thermogenesis (NST) was evaluated by norepinephrine (NE) injection. Compared to PBS treated Ucp1-DTR mice, DT treated Ucp1-DTR mice show a significant impairment in NST (Figure S5B and C). The injection of DT covered the entire reproductive stage in Ucp1-DTR group and age-matched wild type group. To avoid any influence of DT on the offspring of Ucp1-DTR mice, all Ucp1-DTR offspring were swapped for wild type offspring and litter size was made equivalent between the two groups (litter size $=$ 8.36 in wild type group and 8.09 in Ucp1-DTR group). The body weight was significantly decreased in Ucp1-DTR lactation mice ($p < 0.05$ by GLM) (Figure S5D). There was also a significant reduction in total food intakes ($p < 0.05$ by GLM) (Figure S5E). Importantly, the litter mass in Ucp1-DTR group was significantly lower ($\sim$18%) than in the control group ($p < 0.05$, by ANOVA) (Figure S5F), but the gross mammary gland tissue weight was not significantly different between the two groups ($p > 0.05$ by ANOVA) (Figure S5G). The milk energy output (MEO) of the Ucp1-DTR group was 15% lower than in the WT group (119 kJ/day vs 103 kJ/day: $F_{1,19} = 5.9$, $p = 0.024$, ANOVA) (Figure S5H).

Taken together, our experiments indicate that both classic brown adipocytes and possibly inguinal beige/brite adipocytes are able to display the mammary basal myoepithelial phenotype *in vivo*. Eliminating these cells appears to have functional impacts on lactation performance.

3.3. Myf5$^+$/Ucp1$^+$ myoepithelial cells express an adipose and myoepithelial signature

To investigate the gene expression signatures of the Myf5$^+$ and Ucp1$^+$ myoepithelial cells, the GFP$^+$ myoepithelial cells (Lin$^-$:CD24$^+$:CD29^{hi}:GFP$^+$) and GFP$^-$ myoepithelial cells (Lin$^-$:CD24$^+$:CD29^{hi}:GFP$^-$) were sorted from the interscapular region of *Myf5-Cre-ROSA*^{mTmG} or *Ucp1-iCre-ROSA*^{mTmG} mice on lactation day 10, and the interscapular mature brown adipocytes were isolated from the 8-week old virgin transgenic mice (Figure S6A and B). FACS combined high throughput RNA-sequencing allow us to analyze the cell type specific gene expression without noise from other unrelated cell types such as stromal or endothelial cells (Table S1). Hierarchical clustering of the differentially expressed genes among the RNA-seq samples is shown in Figure 3A and Table S2. The main differentially expressed genes were between the brown adipocytes and the myoepithelial cells. The Myf5$^+$ and Ucp1$^+$ myoepithelial cell gene

expression profiles were distinct from the Myf5$^-$ and Ucp1$^-$ myoepithelial cells. This included lower levels of the adipose markers (e.g., *Plin1*, *Adipoq*, and *Retn*) and the browning markers (e.g., *Cox8b* and *Ppargc1a*), but *Ucp1* was only expressed in the brown adipocyte groups. The smooth muscle associated genes (e.g., *Acta2*, *Tagln*, *Cnn1*, and *Myh11*) and the myoepithelial cell associated genes (e.g., *Krt14* and *Krt5*) were enriched in the Myf5$^+$ and Ucp1$^+$ myoepithelial cells in contrast to the Myf5$^+$ and Ucp1$^+$ brown adipocytes (Figure 3C and D and Table S3). This pattern is also supported by recent studies showing that Acta2$^+$ [9,40–42] and Myh11$^+$ [43] smooth muscle-like cells are able to differentiate into beige/brite adipocytes under certain circumstances. The beige adipocyte marker *Ebf2* [44,45] and the pericyte markers *Pdgfra* [46] and *Pdgfrb* [47], which are tightly linked to beige adipocyte differentiation, are also enriched in the Myf5$^+$/Ucp1$^+$ myoepithelial cells. RNA-seq data suggested that the GFP$^+$ myoepithelial cells carried a mix of both smooth muscle-like and adipose-like signatures, when compared to GFP$^+$ brown adipocytes and GFP$^-$ myoepithelial cells respectively (Figure 3C). Selected gene expression was validated by qPCR (Figure 3D).

3.4. Mammary-derived epithelial cells can display adipose features after weaning

We found that brown preadipocytes/adipocytes displayed a mammary basal myoepithelial cell phenotype during the reproductive stage. We next asked whether mammary-derived cells could display an adipocyte phenotype after weaning was completed and the mammary gland involuted. *Krt14-Cre-ROSA^{mTmG}* mice were bred by crossing *Krt14-Cre* mice with *Rosa-mTmG* reporter mice. The Krt14-GFP anterior mammary gland did not express the adipose marker Perilipin1 or contain lipid droplets (LipidTox) in the virgin and lactation period (Figure 4A and B, S7A and B). Five days after weaning, the *Krt14-Cre-ROSA^{mTmG}* mice were exposed to 5 °C cold stimulation for 4 days. Immunostaining in BAT confirmed that Krt14-GFP cells were Perilipin1 and UCP1 positive in the interscapular region, suggesting that, on average, 0.8% brown adipocytes were converted from mammary epithelial cells (Figures 4C and D and S7D). The Krt14-GFP positive cells were also observed to have lipid droplets in the inguinal subcutaneous adipose fat pad (Figure S7C). One possible explanation for the adipocytes expressing the Krt14-GFP signal is the adipose-derived mammary cells revert back to their adipose phenotype after lactation. A second possibility is that some Krt14-derived mammary cells responded to the strong post-partum adipogenic microenvironmental stimulation [48].

Supporting the *in vivo* work, we explored whether Krt14-positive myoepithelial cells could differentiate into adipocytes *in vitro*. We cultured inguinal Krt14$^+$ SVF cells from the virgin *Krt14-Cre-ROSA^{mTmG}* mice in adipogenic conditions for 6 days, and Krt14$^+$ cells produced lipid droplets and were PPAR-γ positive (Figure 4E–G). Furthermore, these Krt14-GFP adipocytes were able to respond to the cAMP signal agonist Forskolin by expressing UCP1 (Figure 4H). This

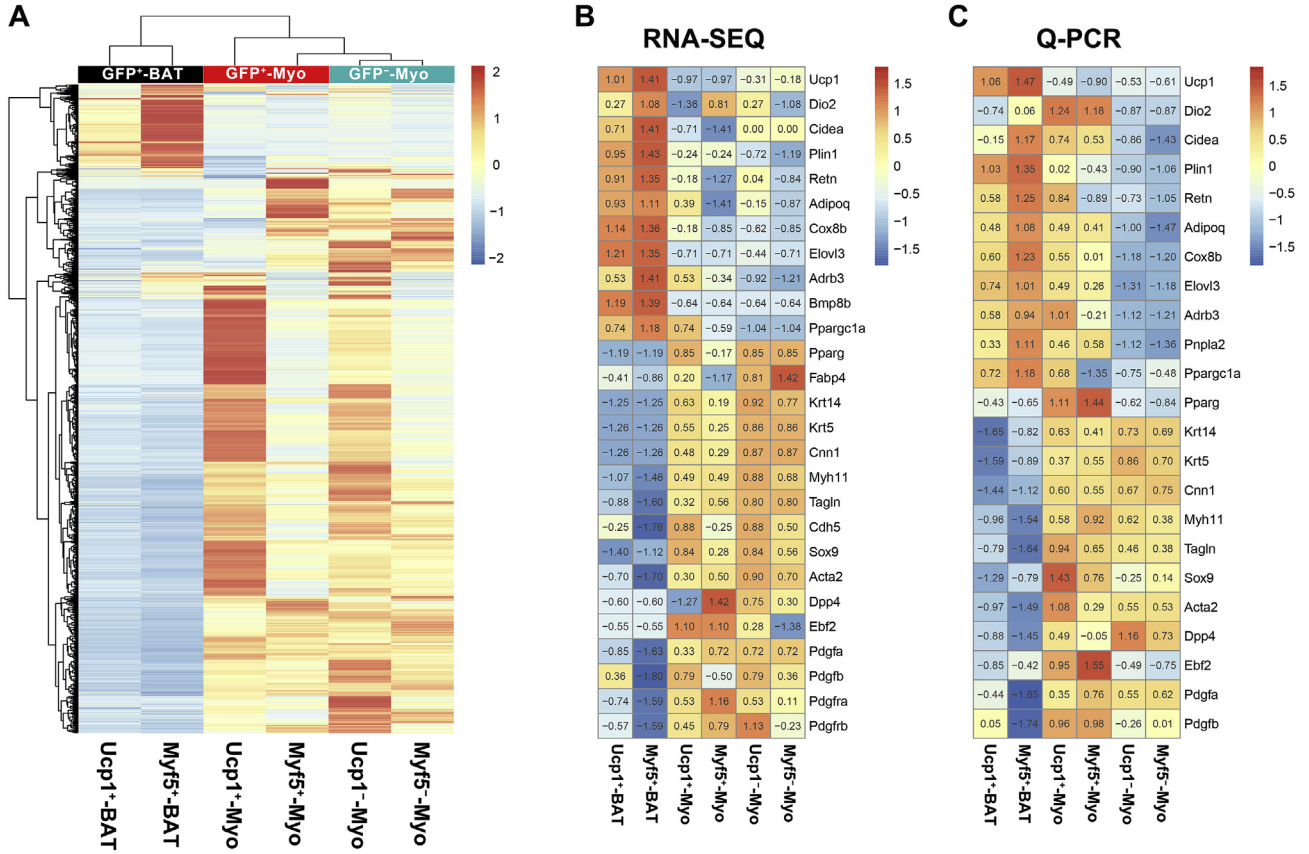

Figure 3: Gene signature of brown origin myoepithelial cells. (A) Hierarchical clustering of the differentially expressed genes from the FACS-Sequencing data set. Rows were clustered using the one minus Pearson correlation distance metric and columns were clustered using the one minus Spearman correlation distance metric. Clustering was performed with the averaged counts for each cell type. (B) Highlighted differentially expressed genes from the Myf5$^+$-Myo group and Ucp1$^+$-Myo group compare to GFP$^+$-BAT and GFP$^-$-Myo groups in the FACS-Sequencing data set. (C) Relative expression by qPCR of the differentially expressed genes from **C** (n = 2 per group). Red and blue indicate relative high and low expression for the row respectively in **A**–**C**.

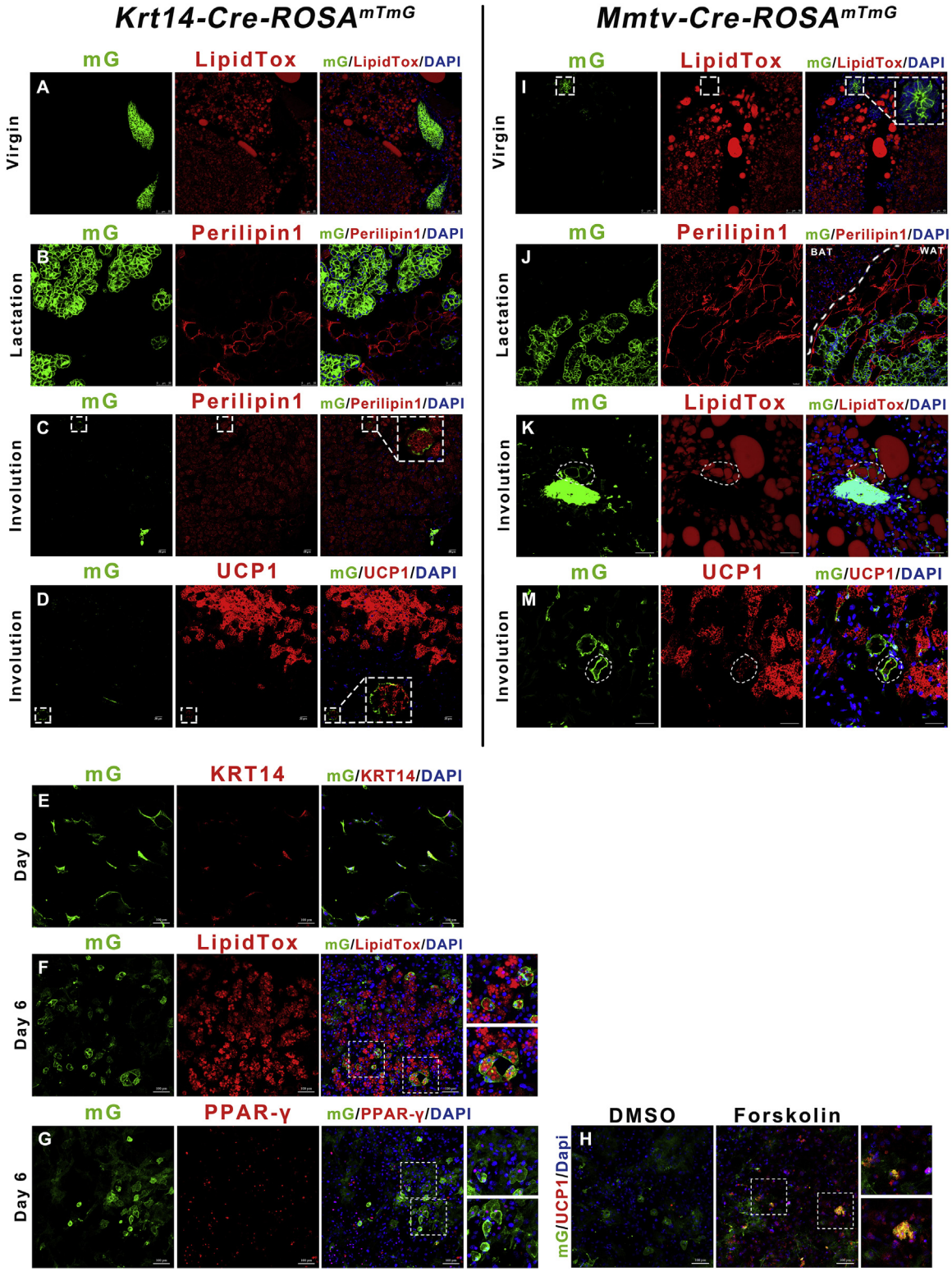

Figure 4: Mammary-derived epithelial cells display adipose features after weaning. (A–D) Interscapular BAT from the virgin, lactation, and involution stages of the *Krt14-Cre-ROSA*^{mTmG} mice were sectioned and immunostained for GFP, Perilipin1, LipidTOX, and UCP1. (E–G) Krt14-GFP SVF cells from *Krt14-Cre-ROSA*^{mTmG} female virgin mice expressed LipidTox (F) and PPAR-γ (G) after 6 days of brown adipogenic stimulation *in vitro*. (H) Differentiated Krt14^{+} adipocytes express UCP1 (right) after 6 h (10 μM) Forskolin treatment. (I–M) Interscapular BAT from virgin, lactation, and involution stages of the *Mmtv-Cre-ROSA*^{mTmG} mice were sectioned and immunostained for GFP, Perilipin1, LipidTOX, and UCP1. Scale bar: 100 μm in E–H and 20 μm in the remaining graphs.

result demonstrates mammary basal myoepithelial cells are able to differentiate into beige/brite-like adipocytes *in vitro*.

To further determine whether Krt14-GFP marked mammary cells display an adipocyte phenotype, we repeated the above experiment using *Mmtv-Cre-ROSA*^{mTmG} mice. The mouse mammary tumor virus (*Mmtv*) promoter driven Cre model is a well-known mouse mammary model [49]. Similar to *Krt14-Cre-ROSA*^{mTmG} mice, the Mmtv-GFP mammary gland cells did not contain lipid droplets in both the virgin and lactation stages (Figures 4I and J, S7E and F). In the post-weaning *Mmtv-Cre-ROSA*^{mTmG} *mice*, Mmtv-GFP cells were observed to be LipidTox and PPAR-γ positive and 1.3% of inguinal adipocytes had a Mmtv origin (Figures 4K and S7G—H). Some of these Mmtv^{+} adipocytes responded to cold exposure with a thermogenic UCP1 signature (Figure 4M).

Overall, these data suggest that mature brown adipocytes are capable of displaying mammary basal myoepithelial features during the reproductive stage, but they do not exhibit a luminal phenotype capable of milk secretion. Beige/brite cells may have a similar capacity. In addition, mammary epithelial cells are capable of exhibiting an adipocyte phenotype, some of which have a browning potential after weaning.

4. DISCUSSION

The previous discovery of a unique lineage of adipocytes that appear able to display both brown and white phenotypes has stimulated considerable interest in the interrelationships between the different adipocyte populations and raised questions whether such cells come from *de novo* recruitment of progenitor cells, or whether all white adipocytes are capable of transdifferentiation. An additional complexity in the interrelationships of the various adipocytes is that previous studies showed that grafted gonadal WAT contributes to the mammary luminal secretory cell population during lactation [19]. However, because this finding was made prior to the discovery of beige/brite adipocytes, it is currently unclear which cell type was responsible for displaying the luminal secretory phenotype. Alternatively, the appearance of apparent transdifferentiation might have been because the 'adipocyte' marker used to identify cells that had a white adipocyte heritage (FABP4^{+}) is not specific to adipocytes [50]. The ability of brown adipocytes to transform into mammary gland cells was previously unknown. We have demonstrated here that brown adipocytes (Ucp1^{+}) contribute to the mammary basal myoepithelial population but not luminal secretory cells. This might be because brown adipocytes come from a skeletal muscle origin (Myf5^{+}), which is more similar to the mammary smooth muscle like basal myoepithelial Krt14^{+} cells, which function to squeeze the milk out of the ducts during milk letdown. However, some previous studies reported that *Myf5* also labels a few white adipocytes in the supra-scapular and inguinal regions [8—10]; therefore, while we were extremely careful to use only tissue from the interscapular region (Figure S1A) and these data are consistent with brown adipocytes transforming to exhibit a myoepithelial phenotype, they are not absolutely definitive. Therefore, we additionally developed *Ucp1-iCre* mouse model combined with *Ucp1-CreER* mouse model, allowing us to definitively separate if the cells were brown or white adipocytes. The *Ucp1-iCre-ROSA*^{mTmG} and *Ucp1-CreER-ROSA*^{tdTomato} mouse model are able to label all mature brown adipocytes, without the white adipocytes in the interscapular region, and the cell tracing of the brown adipocytes by the injection of DIO-AAV before lactation and the Ucp1-GFP cell graft experiment confirm that active mature brown adipocytes can convert into mammary myoepithelial cell during gestation period.

The adipose microenvironment is crucial for the activation of UCP1 and maintenance of the browning capability [11]. During the reproductive period, the essential hormones of mammary development and maturation (such as prolactin), as well as hormones reflecting body composition (such as leptin) are correlated with UCP1 in BAT [24]. Mice lacking prolactin receptor were protected from high fat diet treatment through browning of their WAT [51]. Furthermore, the well-known brown specific gene *Cidea* has been found to regulate the mammary gland milk secretion as a coactivator of C/EBPβ [52], but it is unknown whether *Cidea* is expressed in the mammary myoepithelial cells during lactation.

We used FACS combined high throughput RNA-seq to analyze the transcriptional pattern of the small proportion of Myf5^{+}/Ucp1^{+} derived mammary myoepithelial cells compared to Myf5^{-}/Ucp1^{-} mammary myoepithelial cells and mature brown adipocytes. The putative Myf5^{+}/Ucp1^{+} mammary myoepithelial cells were enriched for smooth muscle genes (albeit at a lower expression level) and some adipose genes compared to Myf5^{-}/Ucp1^{-} mammary myoepithelial cells consistent with the Myf5^{+}/Ucp1^{+} mammary myoepithelial cells being converted brown adipocytes. Interestingly, the basal myoepithelial population (Lin^{-}:CD24^{+}:CD29^{hi}) revealed some genes (e.g., *Krt8* and *Csn2*) typically associated with luminal cells in the RNA-seq result. We further combined KRT14 and KRT8 with the cell surface markers to study the distribution of the mammary lineage cells. KRT14 is loyally expressed in the basal myoepithelial population (Lin^{-}:CD24^{+}:CD29^{hi}) in both virgin and lactation state (Figure S6C). On the contrary, KRT8 is expressed in basal (Lin^{-}:CD24^{+}:CD29^{hi}) and luminal (Lin^{-}:CD24^{+}:CD29^{lo}) population during lactation state (Figure S6D). It is possible that the microenvironment of lactation state influenced the CD29 level of the luminal population. There are also recent studies suggesting the bipotential (e.g., Krt14^{+}, α-SMA^{+}) basal myoepithelial lineage progenitor cells can contribute to both myoepithelial and luminal cells in the lactation state [14,53—55] which involves some myoepithelium-like Ucp1-RFP cells in the *Ucp1-CreER-ROSA*^{tdTomato} mouse model carrying both Krt14 and Krt8. Nonetheless FACS sorting excluded the majority of cell contamination such as stromal or endothelial or immune cells in the further GFP^{+} versus GFP^{-} mammary cells transcriptional analysis. Furthermore, no KRT8 signal was observed in the Myf5-GFP or Ucp1-GFP cells by the immunostaining analysis (Figures 1D and 2D) in *Myf5-Cre-ROSA*^{mTmG} and *Ucp1-iCre-ROSA*^{mTmG} mice models. Interestingly, the Perilipin1 negative Ucp1-RFP cells were UCP1 positive in the interscapular region but UCP1 negative in the inguinal mammary gland (Figure S4D and F), which is similar to the Ucp1-GFP adipocytes graft experiment. Different from the *Ucp1-iCre* model, around 37% Perilipin1 negative slender Ucp1-RFP cells expressed the mammary luminal marker KRT8 (Figure S4E—G) without typical luminal morphology, which indicates that the Ucp1-RFP cells might be bipotential. The putative brown derived (Myf5^{+}/Ucp1^{+}) myoepithelial cells (Lin^{-}:CD24^{+}:CD29^{hi}) showed a myoepithelial cell phenotype and markers.

Although the population of cells that originate as brown adipocytes and then show a mammary myoepithelial cell phenotype in lactation is small (less than 5% of myoepithelial cells), this population may be functionally important in milk expression from the mammary gland because when these specific cells were killed by diphtheria toxin in Ucp1-DTR mice during lactation, there was a significant impact on milk production and growth of the offspring. Of course the DT in these mice would also kill all the brown adipocytes as well as preventing any adipoctyes from converting to myoepithelial cells. A negative impact on lactation may then come about because of the lack of brown adipocytes. This seems unlikely, however, because *a priori*, one might expect the opposite

result of killing brown adipocytes in lactation. Previous work has shown that during lactation, mouse milk production is limited by capacity to dissipate heat [56,57]. This explains why UCP1 is downregulated during lactation [24,25], to minimize competitive heat production. Completely eliminating UCP1 expressing cells in lactation might then be predicted to enhance milk production and pup growth if these cells had no additional purpose, such as contributing to mammary gland function.

We also demonstrated that mammary epithelial cells (Krt14$^+$ and Mmtv$^+$) could display an adipose phenotype after weaning, which was established using the current *Krt14-Cre-ROSA^{mTmG}* and *Mmtv-Cre-ROSA^{mTmG}* models. It has been previously indicated that vascular smooth muscle (Myh11$^+$ and α-SMA$^+$) lineage cells [41,43] and pericyte lineage (PDGFR-α^+) cells [46,58] can give rise to adipocytes. Yet, other studies show that Myh11$^+$ or α-SMA$^+$ [53] lineage cells also give rise to mammary basal myoepithelial cells. We chose the *Krt14-Cre-ROSA^{mTmG}* and *Mmtv-Cre-ROSA^{mTmG}* strategy to test the sole role of mammary epithelial cells without labeling vascular cells in the process. Furthermore, it was possible to differentiate Krt14$^+$ SVF cells into adipocytes with thermogenic features at the cellular level, and animal models further confirmed this phenotype. Nevertheless, it was still unclear whether the undifferentiated myoepithelial stem cells or differentiated myoepithelial cells or both were involved in this cellular fate conversion. In a previous 'browning' mouse model, chronic overexpression of oncogene Cyclooxygenase2 (COX2) [59] or Son of Sevenless (SOS) [60], driven by the skin/mammary myoepithelial promoter Krt5, increased energy expenditure and induced a browning phenotype at room temperature, indicating that the myoepithelial cells could accumulate lipid and activate UCP1 expression under special conditions. Moreover, the brown/beige cell marker UCP1 expressed in the Breast Cancer Susceptibility gene-1 (Brca1) mutant breast cancer model [61] and the substantial reactive oxygen species (ROS) production could regulate the UCP1-dependent thermogenesis [62], suggesting that the uncoupling process might play a critical role in the redox balance and ROS production in cancer cells [63]. Recent studies indicate the cachectic lipolysis and lipogenesis in stromal WAT occurs in a UCP1-independent manner [64]. However, it is still unclear whether the dissipation of proton gradient in the mitochondria by UCP1 is favorable for tumor growth, which requires further investigation. In our study, the activation of UCP1 in brown/beige adipocytes was achieved via cold stimulation. Based on previous myoepithelial cells models [59,60], it is possible to activate UCP1 expression in myoepithelial cells via either a robust pharmacological (e.g., CL-316243) or pathological (e.g., breast cancer) manner. Hence, in the non-breeding and nonpathologic stage, mammary basal myoepithelial cells may potentially be recruited as a source of beige/brite adipocytes.

5. CONCLUSION

Collectively, our lineage-tracing data show that both a small proportion brown adipocytes (Ucp1$^+$) and beige/brite adipocytes (Ucp1$^{-/+}$) are able to display a mammary basal myoepithelial cell phenotype but not a luminal cell phenotype. We also demonstrate that, after weaning, a small proportion of mammary epithelial cells contribute to the adipocyte pool that can show a thermogenic signature. These changes may make a significant contribution to mammary gland function.

AUTHORS' CONTRIBUTION

Conceptualization, J.R.S.; Methodology, L.L., B.G.L.; Investigation, L.L., B.G.L., M.L., C.Q.N., G.L.W., T.L., E.K., Writing — Original Draft, L.L., B.G.L., J.R.S.; Writing — Review& Editing, L.L., B.G.L., E.K., W.Z.J., J.R.S.; Supervision, J.R.S.

ACKNOWLEDGEMENTS

This work was supported by the Strategic Priority Research Program of the Chinese Academy of Sciences (XDB13030000) and the CAS-Novonordisk Foundation, as well as grants from the '1000 talents' recruitment program, and a 'Great-wall professorship' from the CAS-Novonordisk Foundation all to JRS. We are grateful to all the members of Molecular Energetics Group for their support and discussion of the results. We would like to thank the Center for Biological Imaging from Institute of Biophysics Chinese Academy of Sciences and Professor Zhaohui Wang's Lab from Institute of Genetics and Developmental Biology Chinese Academy of Sciences for confocal microscopy and the Center for Developmental Biology from Institute of Genetics and Developmental Biology Chinese Academy of Sciences and Dr. Jai from Core Facility for Protein Research from Institute of Biophysics Chinese Academy of Sciences for flow cytometry. We are grateful to Dr. Kuang from Purdue University and Dr. Zhu from Chinese Academy of Medical Sciences Peking Union Medical College for the kind donation of Myf5-Cre mice and Dr. Wolfrum from the Institute of Food Nutrition and Health at the ETH Zurich for the kind donation of the Ucp1-DTR mice. Xun Huang provided valuable comments on previous versions of the manuscript.

CONFLICTS OF INTEREST

The authors declare no conflict of interest.

APPENDIX A. SUPPLEMENTARY DATA

Supplementary data related to this article can be found at http://dx.doi.org/10.1016/j.molmet.2017.07.015.

REFERENCES

[1] Cannon, B., Nedergaard, J., 2004. Brown adipose tissue: function and physiological significance. Physiological Reviews 84:277—359.

[2] Petrovic, N., Walden, T.B., Shabalina, I.G., Timmons, J.A., Cannon, B., Nedergaard, J., 2010. Chronic peroxisome proliferator-activated receptor gamma (PPARgamma) activation of epididymally derived white adipocyte cultures reveals a population of thermogenically competent, UCP1-containing adipocytes molecularly distinct from classic brown adipocytes. Journal of Biological Chemistry 285:7153—7164.

[3] Wu, J., Bostrom, P., Sparks, L.M., Ye, L., Choi, J.H., Giang, A.H., et al., 2012. Beige adipocytes are a distinct type of thermogenic fat cell in mouse and human. Cell 150:366—376.

[4] Seale, P., Bjork, B., Yang, W., Kajimura, S., Chin, S., Kuang, S., et al., 2008. PRDM16 controls a brown fat/skeletal muscle switch. Nature 454:961—967.

[5] Timmons, J.A., Wennmalm, K., Larsson, O., Walden, T.B., Lassmann, T., Petrovic, N., et al., 2007. Myogenic gene expression signature establishes that brown and white adipocytes originate from distinct cell lineages. Proceedings of the National Academy of Sciences of the United States of America 104:4401—4406.

[6] Lepper, C., Fan, C.M., 2010. Inducible lineage tracing of Pax7-descendant cells reveals embryonic origin of adult satellite cells. Genesis 48:424—436.

[7] Joe, A.W.B., Yi, L., Natarajan, A., Le Grand, F., So, L., Wang, J., et al., 2010. Muscle injury activates resident fibro/adipogenic progenitors that facilitate myogenesis. Nature Cell Biology 12:153—163.

[8] Sanchez-Gurmaches, J., Hung, C.M., Sparks, C.A., Tang, Y., Li, H., Guertin, D.A., 2012. PTEN loss in the Myf5 lineage redistributes body fat and reveals subsets of white adipocytes that arise from Myf5 precursors. Cell Metabolism 16:348—362.

[9] Berry, D.C., Jiang, Y., Graff, J.M., 2016. Mouse strains to study cold-inducible beige progenitors and beige adipocyte formation and function. Nature Communication 7:10184.

[10] Sanchez-Gurmaches, J., Guertin, D.A., 2014. Adipocytes arise from multiple lineages that are heterogeneously and dynamically distributed. Nature Communication 5:4099.

[11] Rosenwald, M., Perdikari, A., Rulicke, T., Wolfrum, C., 2013. Bi-directional interconversion of brite and white adipocytes. Nature Cell Biology 15:659–667.

[12] Sternlicht, M.D., 2006. Key stages in mammary gland development: the cues that regulate ductal branching morphogenesis. Breast Cancer Research 8:201.

[13] Deugnier, M.-A., Teulière, J., Faraldo, M.M., Thiery, J.P., Glukhova, M.A., 2002. The importance of being a myoepithelial cell. Breast Cancer Research 4:224.

[14] Van Keymeulen, A., Rocha, A.S., Ousset, M., Beck, B., Bouvencourt, G., Rock, J., et al., 2011. Distinct stem cells contribute to mammary gland development and maintenance. Nature 479:189–193.

[15] Stingl, J., Eirew, P., Ricketson, I., Shackleton, M., Vaillant, F., Choi, D., et al., 2006. Purification and unique properties of mammary epithelial stem cells. Nature 439:993–997.

[16] Hennighausen, L., Robinson, G.W., 2005. Information networks in the mammary gland. Nature Reviews: Molecular Cell Biology 6:715–725.

[17] Gjorevski, N., Nelson, C.M., 2011. Integrated morphodynamic signalling of the mammary gland. Nature Reviews: Molecular Cell Biology 12:581–593.

[18] Morroni, M., Giordano, A., Zingaretti, M.C., Boiani, R., De Matteis, R., Kahn, B.B., et al., 2004. Reversible transdifferentiation of secretory epithelial cells into adipocytes in the mammary gland. Proceedings of the National Academy of Sciences of the United States of America 101: 16801–16806.

[19] De Matteis, R., Zingaretti, M.C., Murano, I., Vitali, A., Frontini, A., Giannulis, I., et al., 2009. *In vivo* physiological transdifferentiation of adult adipose cells. Stem Cells 27:2761–2768.

[20] Giordano, A., Smorlesi, A., Frontini, A., Barbatelli, G., Cinti, S., 2014. White, brown and pink adipocytes: the extraordinary plasticity of the adipose organ. European Journal of Endocrinology of the European Federation of Endocrine Societies 170:R159–R171.

[21] Singh, R., Parveen, M., Basgen, J.M., Fazel, S., Meshesha, M.F., Thames, E.C., et al., 2016. Increased expression of beige/brown adipose markers from host and breast cancer cells influence xenograft formation in mice. Molecular Cancer Research 14:78–92.

[22] Shackleton, M., Vaillant, F., Simpson, K.J., Stingl, J., Smyth, G.K., Asselin-Labat, M.L., et al., 2006. Generation of a functional mammary gland from a single stem cell. Nature 439:84–88.

[23] Jackson, D.M., Hambly, C., Trayhurn, P., Speakman, J.R., 2001. Can non-shivering thermogenesis in brown adipose tissue following NA injection be quantified by changes in overlying surface temperatures using infrared thermography? Journal of Thermal Biology 26:85–93.

[24] Krol, E., Martin, S.A., Huhtaniemi, I.T., Douglas, A., Speakman, J.R., 2011. Negative correlation between milk production and brown adipose tissue gene expression in lactating mice. Journal of Experimental Biology 214: 4160–4170.

[25] Trayhurn, P., Douglas, J.B., Mcguckin, M.M., 1982. Brown adipose tissue thermogenesis is suppressed during lactation in mice. Nature 298:59–60.

[26] Rudnicki, M.A., Schnegelsberg, P.N.J., Stead, R.H., Braun, T., Arnold, H.H., Jaenisch, R., 1993. MyoD or Myf5 is required for the formation of skeletal muscle. Cell 75:1351–1359.

[27] Tallquist, M.D., Weismann, K.E., Hellstrom, M., Soriano, P., 2000. Early myotome specification regulates PDGFA expression and axial skeleton development. Development 127:5059–5070.

[28] Sanchez-Gurmaches, J., Guertin, D.A., 2014. Adipocyte lineages: tracing back the origins of fat. Biochimica et Biophysica Acta 1842:340–351.

[29] Shan, T., Liang, X., Bi, P., Zhang, P., Liu, W., Kuang, S., 2013. Distinct populations of adipogenic and myogenic Myf5-lineage progenitors in white adipose tissues. Journal of Lipid Research 54:2214–2224.

[30] Schulz, T.J., Huang, T.L., Tran, T.T., Zhang, H., Townsend, K.L., Shadrach, J.L., et al., 2011. Identification of inducible brown adipocyte progenitors residing in skeletal muscle and white fat. Proceedings of the National Academy of Sciences of the United States of America 108:143–148.

[31] Muzumdar, M.D., Tasic, B., Miyamichi, K., Li, L., Luo, L., 2007. A global double-fluorescent Cre reporter mouse. Genesis 45:593–605.

[32] Galmozzi, A., Sonne, S.B., Altshuler-Keylin, S., Hasegawa, Y., Shinoda, K., Luijten, I.H., et al., 2014. ThermoMouse: an in vivo model to identify modulators of UCP1 expression in brown adipose tissue. Cell Reports 9: 1584–1593.

[33] Park, A., Kim, W.K., Bae, K.H., 2014. Distinction of white, beige and brown adipocytes derived from mesenchymal stem cells. World Journal of Stem Cells 6:33–42.

[34] Talmadge, J.E., Meyers, K.M., Prieur, D.J., Starkey, J.R., 1980. Role of NK cells in tumour growth and metastasis in beige mice. Nature 284: 622–624.

[35] Bosma, G.C., Custer, R.P., Bosma, M.J., 1983. A severe combined immunodeficiency mutation in the mouse. Nature 301:527–530.

[36] Liu, X., Zheng, Z., Zhu, X., Meng, M., Li, L., Shen, Y., et al., 2013. Brown adipose tissue transplantation improves whole-body energy metabolism. Cell Research 23:851–854.

[37] Tran, T.T., Kahn, C.R., 2010. Transplantation of adipose tissue and stem cells: role in metabolism and disease. Nature Reviews: Endocrinology 6:195–213.

[38] Stanford, K.I., Middelbeek, R.J., Townsend, K.L., An, D., Nygaard, E.B., Hitchcox, K.M., et al., 2013. Brown adipose tissue regulates glucose homeostasis and insulin sensitivity. Journal of Clinical Investigation 123: 215–223.

[39] Liu, X., Wang, S., You, Y., Meng, M., Zheng, Z., Dong, M., et al., 2015. Brown adipose tissue transplantation reverses obesity in Ob/Ob Mice. Endocrinology 156:2461–2469.

[40] Berry, D.C., Jiang, Y., Arpke, R.W., Close, E.L., Uchida, A., Reading, D., et al., 2017. Cellular aging contributes to failure of cold-induced beige adipocyte formation in old mice and humans. Cell Metabolism 25:166–181.

[41] Jiang, Y., Berry, D.C., Tang, W., Graff, J.M., 2014. Independent stem cell lineages regulate adipose organogenesis and adipose homeostasis. Cell Reports 9:1007–1022.

[42] Berry, D.C., Jiang, Y., Graff, J.M., 2016. Emerging roles of adipose progenitor cells in tissue development, homeostasis, expansion and thermogenesis. Trends in Endocrinology and Metabolism 27:574–585.

[43] Long, J.Z., Svensson, K.J., Tsai, L., Zeng, X., Roh, H.C., Kong, X., et al., 2014. A smooth muscle-like origin for beige adipocytes. Cell Metabolism 19:810–820.

[44] Rajakumari, S., Wu, J., Ishibashi, J., Lim, H.W., Giang, A.H., Won, K.J., et al., 2013. EBF2 determines and maintains brown adipocyte identity. Cell Metabolism 17:562–574.

[45] Wang, W., Kissig, M., Rajakumari, S., Huang, L., Lim, H.W., Won, K.J., et al., 2014. Ebf2 is a selective marker of brown and beige adipogenic precursor cells. Proceedings of the National Academy of Sciences of the United States of America 111:14466–14471.

[46] Lee, Y.H., Petkova, A.P., Mottillo, E.P., Granneman, J.G., 2012. In vivo identification of bipotential adipocyte progenitors recruited by beta3-adrenoceptor activation and high-fat feeding. Cell Metabolism 15:480–491.

[47] Vishvanath, L., MacPherson, K.A., Hepler, C., Wang, Q.A., Shao, M., Spurgin, S.B., et al., 2016. Pdgfrbeta+ mural preadipocytes contribute to adipocyte hyperplasia induced by high-fat-diet feeding and prolonged cold exposure in adult mice. Cell Metabolism 23:350–359.

[48] Silberstein, G.B., 2001. Postnatal mammary gland morphogenesis. Microscopy Research and Technique 52:155–162.

[49] Wagner, K.U., Wall, R.J., St-Onge, L., Gruss, P., Wynshaw-Boris, A., Garrett, L., et al., 1997. Cre-mediated gene deletion in the mammary gland. Nucleic Acids Research 25:4323–4330.

[50] Jeffery, E., Berry, R., Church, C.D., Yu, S., Shook, B.A., Horsley, V., et al., 2014. Characterization of Cre recombinase models for the study of adipose tissue. Adipocyte 3:206–211.

[51] Auffret, J., Viengchareun, S., Carre, N., Denis, R.G., Magnan, C., Marie, P.Y., et al., 2012. Beige differentiation of adipose depots in mice lacking prolactin receptor protects against high-fat-diet-induced obesity. FASEB Journal 26: 3728–3737.

[52] Wang, W.S., Lv, N., Zhang, S.S., Shui, G.H., Qian, H., Zhang, J.F., et al., 2012. Cidea is an essential transcriptional coactivator regulating mammary gland secretion of milk lipids. Nature Medicine 18:235–243.

[53] Prater, M.D., Petit, V., Alasdair Russell, I., Giraddi, R.R., Shehata, M., Menon, S., et al., 2014. Mammary stem cells have myoepithelial cell properties. Nature Cell Biology 16:942–950, 941–947.

[54] Rios, A.C., Fu, N.Y., Lindeman, G.J., Visvader, J.E., 2014. In situ identification of bipotent stem cells in the mammary gland. Nature 506:322–327.

[55] Scheele, C.L., Hannezo, E., Muraro, M.J., Zomer, A., Langedijk, N.S., van Oudenaarden, A., et al., 2017. Identity and dynamics of mammary stem cells during branching morphogenesis. Nature 542:313–317.

[56] Krol, E., Speakman, J.R., 2003. Limits to sustained energy intake VII. Milk energy output in laboratory mice at thermoneutrality. Journal of Experimental Biology 206:4267–4281.

[57] Krol, E., Murphy, M., Speakman, J.R., 2007. Limits to sustained energy intake. X. Effects of fur removal on reproductive performance in laboratory mice. Journal of Experimental Biology 210:4233–4243.

[58] Berry, R., Rodeheffer, M.S., 2013. Characterization of the adipocyte cellular lineage in vivo. Nature Cell Biology 15:302–308.

[59] Vegiopoulos, A., Muller-Decker, K., Strzoda, D., Schmitt, I., Chichelnitskiy, E., Ostertag, A., et al., 2010. Cyclooxygenase-2 controls energy homeostasis in mice by de novo recruitment of brown adipocytes. Science 328:1158–1161.

[60] Petruzzelli, M., Schweiger, M., Schreiber, R., Campos-Olivas, R., Tsoli, M., Allen, J., et al., 2014. A switch from white to brown fat increases energy expenditure in cancer-associated cachexia. Cell Metabolism 20:433–447.

[61] Jones, L.P., Buelto, D., Tago, E., Owusu-Boaitey, K.E., 2011. Abnormal mammary adipose tissue environment of Brca1 mutant mice show a persistent deposition of highly vascularized multilocular adipocytes. Journal of Cancer Science & Therapy 004.

[62] Chouchani, E.T., Kazak, L., Jedrychowski, M.P., Lu, G.Z., Erickson, B.K., Szpyt, J., et al., 2016. Mitochondrial ROS regulate thermogenic energy expenditure and sulfenylation of UCP1. Nature 532:112–116.

[63] Sabharwal, S.S., Schumacker, P.T., 2014. Mitochondrial ROS in cancer: initiators, amplifiers or an Achilles' heel? Nature Reviews: Cancer 14:709–721.

[64] Rohm, M., Schafer, M., Laurent, V., Ustunel, B.E., Niopek, K., Algire, C., et al., 2016. An AMP-activated protein kinase-stabilizing peptide ameliorates adipose tissue wasting in cancer cachexia in mice. Nature Medicine 22:1120–1130.

